The relaxation rate of a stochastic spreading process in a closed ring

Daniel Hurowitz, Doron Cohen
Department of Physics, Ben-Gurion University of the Negev, Beer-Sheva, Israel

The relaxation process of a diffusive ring becomes under-damped if the bias (so called affinity) exceeds a critical threshold value. This is related to the spectral properties of the pertinent stochastic kernel, aka delocalization transition. We find the dependence of the relaxation rate on the affinity and on the length of the ring. Additionally we study the implications of introducing a weak-link into the circuit, and illuminate some subtleties that arise while taking the continuum limit of the discrete model.

I. INTRODUCTION

In the absence of topology the relaxation time of a stochastic sample is either diffusion limited or drift limited, depending on whether the bias is small or large, respectively. However, in a topologically closed circuit, as the bias is increased, the relaxation spectrum becomes complex and the relaxation-rate becomes diffusion-limited rather than drift-limited. In related applications the "circuit" might be a chemical-cycle, and the "bias" is the so called *affinity* of the cycle.

In the present work we consider a minimal model for a topologically closed circuit, namely, an N site ring with nearest-neighbor hopping. The dynamics can be regarded as a stochastic process in which a particle hops from site to site. The rate equation for the site occupation probabilities $\boldsymbol{p} = \{p_n\}$ can be written in matrix notation as

$$\frac{d\boldsymbol{p}}{dt} = \boldsymbol{W}\boldsymbol{p}, \tag{1}$$

If the ring were opened, then the $N \to \infty$ limit would correspond to Sinai's spreading problem [1–4], aka *a random walk in a random environment*, where the transition rates are allowed to be asymmetric. Such models have diverse applications, notably in biophysical contexts of populations biology [5, 6] pulling pinned polymers and DNA unzipping [7, 8] and in particular with regard to molecular motors [9–12].

In the absence of topology $\boldsymbol{W}$ is *similar* to a real symmetric matrix, and the relaxation spectrum is *real*. Alas, for a ring the affinity is a topological-invariant that cannot be gauged away, analogous to the Aharonov-Bohm flux. Thus the theme that we are addressing here is related to the study of of non-Hermitian quantum Hamiltonians [13–15]. In a previous work [16] we have illuminated the relation between the sliding-transition and the complexity-threshold, aka "de-localization transition", as the affinity is increased.

The outline is as follows: In Sec.II we discuss the relaxation in the case of an homogeneously disordered diffusive sample, contrasting non-trivial topology (ring) with simple geometry (box). The effect of disorder is demonstrated in Sec.III, and heuristic considerations are used in order to explain the dependence of the relaxation rate on the affinity and on the length of the ring. In Sec.IV we discuss the delocalization transition. Namely, we find the threshold value of the affinity beyond which the relaxation becomes under-damped. Then we extract the relaxation rate from the characteristic equation using an "electrostatic picture". Sections V and VI concern a ring that has an additional weak-link that forms a bottleneck for diffusion, though not blocking it completely. Several appendices are provided to make the presentation self-contained.

II. DIFFUSIVE SAMPLE: RING VS BOX

The rate equation Eq. (1) involves a matrix $\boldsymbol{W}$ whose off-diagonal elements are the transition rates w_{nm}, and whose diagonal elements are $-\gamma_n$ such that each column sums to zero. For a clean ring and with near-neighbor hopping, the rates are uniform but asymmetric, and are equal to $\overrightarrow{w} = we^{s/2}$ for forward hopping, and $\overleftarrow{w} = we^{-s/2}$ for backward hopping. The $\boldsymbol{W}$ matrix takes the form

$$\boldsymbol{W} = \begin{bmatrix} -\gamma & \overleftarrow{w} & 0 & \dots \\ \overrightarrow{w} & -\gamma & \overleftarrow{w} & \dots \\ 0 & \overrightarrow{w} & -\gamma & \dots \\ \dots & \dots & \dots & \dots \end{bmatrix} \tag{2}$$

with $\gamma = -2w\cosh(s/2)$. Due to translational invariance, the matrix $\boldsymbol{W}$ can be written in terms of momentum operators

$$\boldsymbol{W} = we^{s/2+i\boldsymbol{P}} + we^{-s/2-i\boldsymbol{P}} - 2w\cosh\left(\frac{s}{2}\right) \tag{3}$$

From here it is easy to see that the eigenvalues $\{-\lambda_\nu\}$ of the $\boldsymbol{W}$ matrix are

$$\lambda_\nu = 2w\ \left[\cosh\left(\frac{s}{2}\right) - \cos\left(\frac{2\pi}{N}\nu + i\frac{s}{2}\right)\right] \tag{4}$$

The non-equilibrium steady state (NESS) is associated with $\lambda_0 = 0$. The complexity of the other eigenvalues implies that the relaxation process in not over-damped. A straightforward analysis of the time-dependent spreading process, see e.g. [17], show that drift velocity and the diffusion coefficient are given by the following expressions:

$$v_0 = (\overrightarrow{w} - \overleftarrow{w})a = 2wa\ \sinh(s/2) \tag{5}$$

$$D_0 = \frac{1}{2}(\overrightarrow{w} + \overleftarrow{w})a^2 = wa^2\ \cosh(s/2) \tag{6}$$

where a is the lattice constant. Note that in Eq. (3) we used the lattice constant as a unit of length ("$a = 1$") else the following replacement is required: $\boldsymbol{P} \mapsto a\boldsymbol{P}$.

It is convenient to consider the continuum limit of the rate equation Eq. (1). In this limit we define $D(x) = wa^2$ and $v(x) = swa$, and the continuity equation for the density $\rho(x_n) = (1/a)p_n$ becomes the Fokker-Planck diffusion equation:

$$\frac{d\rho}{dt} \;=\; -\frac{d}{dx}\left[-D(x)\frac{d\rho}{dx} + v(x)\rho(x)\right] \tag{7}$$

One can easily find the spectrum of the relaxation modes ($\lambda_n > 0$) for either "ring" or "box" geometry. The boundary conditions are respectively either of Neumann type or periodic. The result is

$$\lambda_\nu[\text{ring}] \;=\; \left(\frac{2\pi}{L}\right)^2 D\nu^2 \;+\; i\frac{2\pi v}{L}\nu \tag{8}$$

$$\lambda_\nu[\text{box}] \;=\; \left(\frac{\pi}{L}\right)^2 D\nu^2 \;+\; \frac{v^2}{4D} \tag{9}$$

where for the ring $\nu = \pm 1, \pm 2, ...$, while for the box $\nu = 1, 2, 3, ...$ Clearly Eq. (8) is consistent with Eq. (4). The relaxation rate Γ is determined by the lowest eigenvalue

$$\Gamma \;\equiv\; \mathrm{Re}[\lambda_1] \tag{10}$$

For the "ring" the result is determined solely by the diffusion coefficient and the length $L = Na$ of the ring:

$$\Gamma[\text{ring}] \;=\; \left(\frac{2\pi}{L}\right)^2 D \tag{11}$$

while for the "box" it becomes drift-limited if the bias is large:

$$\Gamma[\text{box}] \;=\; \left[\left(\frac{\pi}{L}\right)^2 + \left(\frac{v}{2D}\right)^2\right] D \tag{12}$$

It is important to realize that in the latter case we have a "gap" in the spectrum, meaning that λ_1 does does not diminish in the $L \to \infty$ limit, hence the relaxation time is finite.

III. DISORDERED RING

In the presence of disorder, the forward and backward rates are random numbers. By considering the long time limit of the time-dependent spreading process it is still possible to define the drift velocity v and diffusion coefficient D. The results depend in an essential way on the affinity of the cycle

$$S_{\circlearrowleft} \;\equiv\; N\, s \tag{13}$$

where s is defined via the sample average

$$\left\langle \ln\left(\frac{\overleftarrow{w}}{\overrightarrow{w}}\right)\right\rangle \;\equiv\; -s \tag{14}$$

Additionally it is useful to define threshold values s_μ via the following expression:

$$\left\langle \left(\frac{\overleftarrow{w}}{\overrightarrow{w}}\right)^\mu\right\rangle \;\equiv\; \mathrm{e}^{-(s-s_\mu)\mu} \tag{15}$$

Here, as in [16–18] we assume that the rates are

$$\overrightarrow{w} \;=\; w\, \mathrm{e}^{+\mathcal{E}_n/2} \tag{16}$$

$$\overleftarrow{w} \;=\; w\, \mathrm{e}^{-\mathcal{E}_n/2} \tag{17}$$

where the "activation energies" $\mathcal{E}_n$ are box distributed within $[s-\sigma, s+\sigma]$. Accordingly the thresholds of Eq. (15) are

$$s_\mu \;=\; \frac{1}{\mu}\ln\left(\frac{\sinh(\sigma\mu)}{\sigma\mu}\right) \tag{18}$$

For small σ one obtains the approximation $s_\mu = (1/6)\mu\sigma^2$ which agrees with the continuum-limit-definition of μ in Eq. (D1).

The relaxation spectrum of a disordered ring can be found numerically by solving the characteristic equation

$$\det(z + \boldsymbol{W}) \;=\; 0 \tag{19}$$

and the relaxation rate is defined as $\Gamma = \mathrm{Re}[\lambda_1]$. For a given realization of disorder we regard $S_{\circlearrowleft}$ as a free parameter. Making $S_{\circlearrowleft}$ larger means that all the $\mathcal{E}_n$ are increased by the the same constant. We define the complexity threshold S_c as the value beyond which the spectrum becomes complex. This means that for $S_{\circlearrowleft} < S_c$ the relaxation is over-damped like in a box, while for $S_{\circlearrowleft} > S_c$ the relaxation is under-damped like in a ring. It has been established [16] that

$$S_c \;=\; N\, s_{1/2} \tag{20}$$

In the upper panel of Fig.1 we calculate the dependence of Γ on $S_{\circlearrowleft}$ for a representative disordered ring via direct diagonalization of the $\boldsymbol{W}$ matrix. We also indicate in the figure the complexity threshold S_c. For sake of comparison we also calculate in the lower panel of Fig.1 the relaxation rate Γ for a box configuration, i.e. one link of the ring has been disconnected. In the latter case the topological aspect is absent and $S_c = \infty$.

First we would like to test whether Eq. (11) and Eq. (12) can be used in order to predict Γ. For this purpose v and D are independently calculated using a standard procedure that is outlined in [17]. Indeed we find a nice agreement.

Having realized that Γ of a ring is determined by D, we would like to understand theoretically the observed non-monotonic variation as a function of s. In the $N \to \infty$ limit the calculation of D can be carried out analytically [2], using equations that are displayed in Appendix A. In this limit $D = 0$ in the range $s < s_{1/2}$ where the spectrum is real; then it becomes infinite for $s_{1/2} < s < s_2$, and finite for $s > s_2$. The result of the calculation in the latter regime is displayed in the figure. As expected it

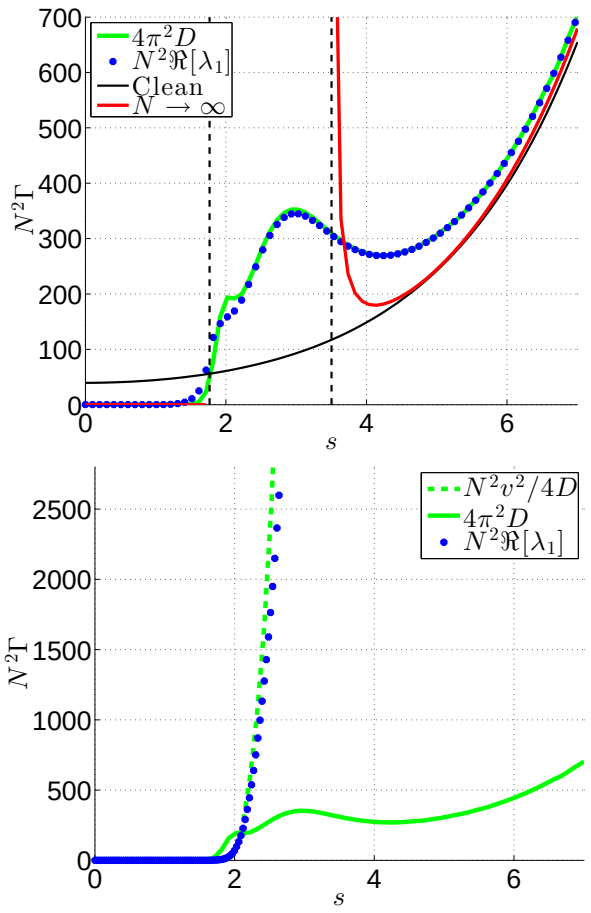

FIG. 1. The relaxation rate $\Gamma = \mathrm{Re}[\lambda_1]$ versus the affinity s for a sample with $N = 1000$ sites, and disorder strength $\sigma = 5$. The upper panel is for a ring, while for the lower panel one bond has been disconnected ("box"). The blue data points have been obtained via numerical diagonalization, whereas the solid and dashed green lines are based on numerically calculated D and v. The lower and upper solid lines in the left panel are based on the analytical estimates of D, namely Eq. (6) and Eq. (A2) respectively. The vertical dashed lines are the thresholds $s_{1/2}$ and s_2.

provides a good estimate only for large s where it can be approximated by Eq. (11) with Eq. (A3), leading to

$$\Gamma \approx \left(\frac{2\pi}{N}\right)^2 \frac{w}{2} \exp\left[\frac{1}{2}s - \frac{3}{2}s_{1/2} + s_1\right] \quad (21)$$

Note that this expression roughly coincides with the clean ring result that is based on Eq. (6). In the range $s_{1/2} < s < s_2$ the diffusion coefficient is large but finite and becomes N dependent. In [18] a heuristic approach has been attempted in order to figure out this N dependence. In the present work we would like to adopt a more rigorous approach. We shall deduce the N dependence of Γ analytically from the characteristic equation Eq. (19). We shall also provide an optional derivation for Eq. (21).

IV. EXTRACTING Γ FROM THE CHARACTERISTIC EQUATION

With the $\boldsymbol{W}$ of the rate equation Eq. (1) it is possible to associate a symmetric real matrix $\boldsymbol{H}$ as explained in Appendix B. The latter has real eigenvalues $-\epsilon_k$ with $k = 0, 1, 2, 3, ...$ Using the identity of Eq. (C3), and setting the units of time such that w=1, the characteristic equation Eq. (19) takes the following form

$$\prod_k (z - \epsilon_k(s)) = (-1)^N 2\left[\cosh\left(\frac{S_{\circlearrowleft}}{2}\right) - 1\right] \quad (22)$$

Taking the log of both sides, this equation takes the form of an electrostatic problem in two dimensions:

$$V(x,y) + iA(x,y) = V(0) \quad (23)$$

where $z = x + iy$. On the left we have a complex potential $\Psi(z)$ of charges that are located along the real axis at ϵ_k. The constant $V(x,y)$ curves correspond to potential contours, and the constant $A(x,y)$ curves corresponds to stream lines. The derivative $\Psi'(z)$ corresponds to the field, which can be regarded as either an electric or a magnetic field up to a 90deg rotation. The identification of the right hand side as $V(0) \equiv V(0,0)$ is based on the observation that $z = \lambda_0 = 0$ has to be an eigenvalue, corresponding to the steady state solution. On the real axis ($x = \epsilon,\ y = 0$), the potential is

$$V(\epsilon) = \sum_k \ln(|\epsilon - \epsilon_k|) \equiv \int \ln(|\epsilon - \epsilon'|)\varrho(\epsilon')d\epsilon' \quad (24)$$

In the electrostatic picture we regard the spectral function $\varrho(\epsilon)$ as a charge distribution. In Appendix E we provide a step by step account of the electrostatic picture to helps gain insight for $V(\epsilon)$. The bottom line is summarized by Fig.2. For full disorder, if $s < s_{1/2}$ the envelope at the origin has a negative slope hence the equations $V(x) = V(0)$ has real solutions, and the relaxation spectrum $\{\lambda_k\}$ comes out real. For $s > s_{1/2}$ the envelope at the origin has a positive slope and the spectrum becomes complex, hence S_c for full disorder is determined by Eq. (20).

We would like to estimate the relaxation rate in the non-trivial regime $S_{\circlearrowleft} > S_c$, where the topology of the ring is reflected. Given the spectral density $\varrho(x)$, the electrostatic potential is

$$V(x,y) = \frac{1}{2}\int \ln\left[(x-x')^2 + y^2\right]\varrho(x')dx' \quad (25)$$

Expanding to second order near the origin, we have

$$V(x,y) \approx C_0 - C_1 x + \frac{1}{2}C_2 y^2 \quad (26)$$

where the coefficients C_n are defined as

$$C_n = \int_0^\infty \frac{1}{\epsilon^n}\varrho(\epsilon)d\epsilon \quad (27)$$

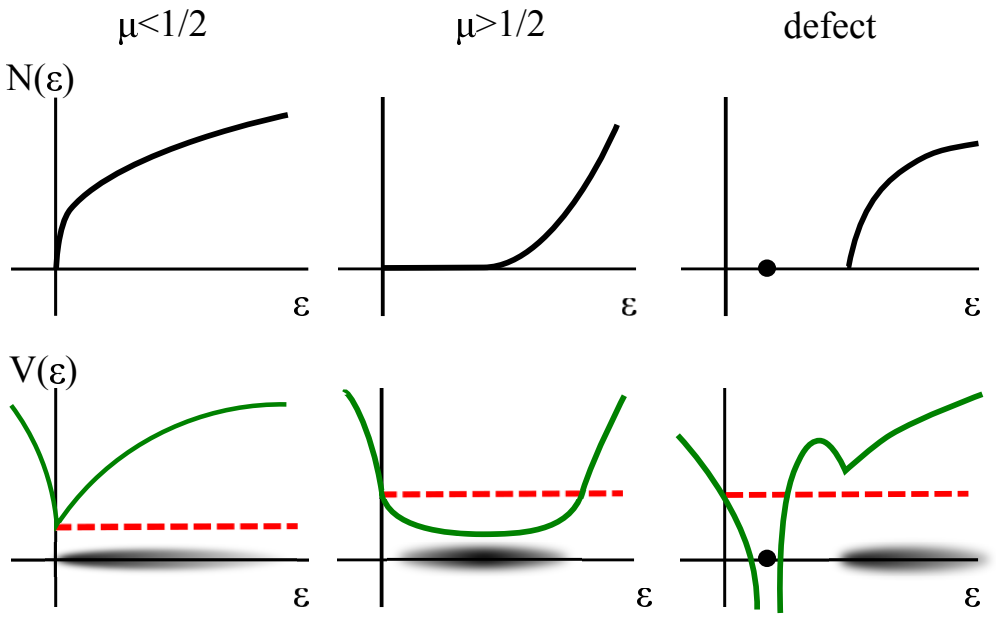

FIG. 2. Caricature of the electrostatic picture used to determine the transition to complexity. The panels of the top row display the integrated density of states that comes from $\varrho(\epsilon)$. The latter is represented by a cloud along the axes of the lower panels. A weak-link contributes an isolated charge at the vicinity of the origin, unlike full disorder that fills the gap with some finite density. The associated envelope of the electrostatic potential is displayed as green lines. The dashed red line is $V(0)$. For $\mu < 1/2$ the equation $V(x) = V(0)$ has real solutions. For $\mu > 1/2$ complex solutions appear.

Notice that $C_0 = V(0)$ and $C_1 = E(0)$ are the potential and the electrostatic field at the origin. To determine the real part of the complex gap it is enough to realize that the equipotential contour $V(x, y) = V(0)$ is approximately a parabola near the origin:

$$x \;=\; \frac{1}{2}\frac{C_2}{C_1}y^2 \tag{28}$$

We define as a reference the field-line $A(x, y) = 0$ that stretches through the origin along the X axis to $-\infty$. The first excited eigenvalue is determined by the intersection of the $V(x, y) = V(0)$ potential contour with the next field line, namely with $A(x, y) = 2\pi$. By definition of the stream function $A(x, y)$, which can be regarded as an application of the Cauchy-Riemann theorem, it is equivalent to the requirement of having an enclosed flux

$$\int_0^{\sqrt{2(C_1/C_2)\Gamma}} \left|\vec{E}(x, y)\right| dy \;=\; 2\pi \tag{29}$$

The integrand is approximated by $|\vec{E}(x, y)| \approx C_1$, hence we deduce

$$\Gamma \;\approx\; 2\pi^2\frac{C_2}{C_1^3} \tag{30}$$

If all the Cs are proportional to N it follows that $\Gamma \propto N^{-2}$ as in the case of a clean diffusive ring. This is indeed the case if $s > s_2$. But if $s < s_2$ we have to be careful about the lower cutoff. From the quantization condition $\mathcal{N}(\epsilon) = 1$ we deduce that $\epsilon_1 \propto N^{-1/\mu}$ and get

$$\Gamma \;\propto\; \begin{cases} N^{-\frac{1}{\mu}} & \text{for } s_{1/2} < s < s_1 \\ N^{-\left(3-\frac{2}{\mu}\right)} & \text{for } s_1 < s < s_2 \\ N^{-2} & \text{for } s > s_2 \end{cases} \tag{31}$$

Comparing with Eq. (11) we realize that consistency requires to assume that $D \propto N^{(2/\mu)-1}$ for $s_1 < s < s_2$, and $D \propto N^{2-(1/\mu)}$ for $s_{1/2} < s < s_1$. The latter result (but not the former) is in agreement with the heuristic approach of [18]. In the heuristic approach it has been assumed, apparently incorrectly, that the disorder-induced correlation-length scales like N throughout the whole regime $s < s_2$, and becomes size-independent for $s > s_2$. Apparently the N dependence of the disorder-induced correlation-length becomes anomalous within the intermediate range $s_1 < s < s_2$.

V. RING WITH WEAK LINK

We would like to analyze how the relaxation spectrum is affected once a weak-link is introduced into a diffusive ring. We use the continuum limit Eq. (7) for the purpose of deriving the characteristic equation. In a region where $v(x)$ and $D(x)$ are constant a free-wave solution $\rho(x) \propto e^{i\tilde{k}x-\lambda t}$, has to satisfy the dispersion relation $\lambda = D\tilde{k}^2 + iv\tilde{k}$. It is convenient to use the notation $s = v/D$, which would be consistent with the discrete-lattice convention if the lattice constant were taken as

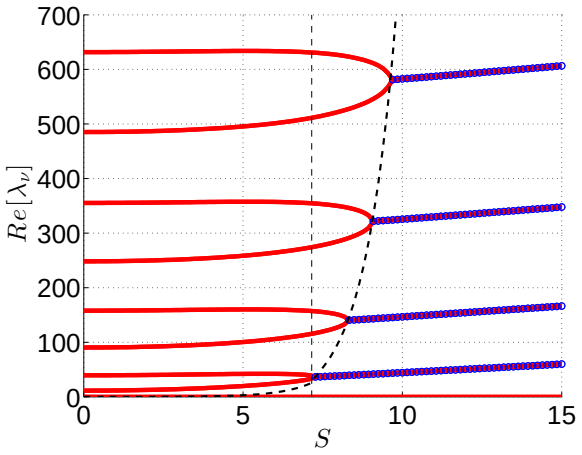

FIG. 3. The lower eignevalues for a ring with a weak link versus S. The units of length and time are such that $D = L = 1$ and we set $g = 0.2$. For large enough $S_\circlearrowleft$ the eigenvalues become complex and the real parts coalesce (indicated by blue circles). The threshold is indicated by the dashed curve that has been deduced from the envelope of the characteristic equation. The dashed vertical lines indicates S_c of Eq. (46).

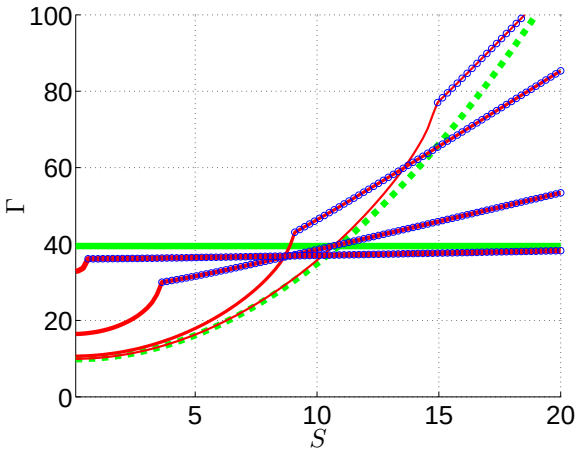

FIG. 4. The relaxation rate Γ for the ring of Fig. 3. The solid lines from bottom to top are for clean ring ($g = \infty$) and for $g = 10, 1, 0.1, 0.01$. To the right of each knee λ_1 becomes complex, indicated by the blue circles. As g decreases, the drift limited value (dashed green line) is approached.

$a = 1$. Given λ we define k that might be either real or pure-imaginary through the following expression:

$$\lambda \equiv \left[k^2 + \left(\frac{s}{2}\right)^2\right] D \tag{32}$$

The complex wavenumbers that correspond to this value are $\tilde{k}_\pm = \pm k - i(s/2)$. In each location the actual stationary solution of Eq. (7) has to be a superposition of clockwise (k_+) and anticlockwise (k_-) waves

$$\rho(x) = \left[Ae^{ikx} + Be^{-ikx}\right] e^{(s/2)x} \tag{33}$$

$$\equiv \psi^+(x) + \psi^-(x) \tag{34}$$

We define the state vector

$$\vec{\psi}(x) \equiv \begin{pmatrix} \rho(x) \\ \partial\rho(x) \end{pmatrix} = \begin{pmatrix} 1 & 1 \\ i\tilde{k}_+ & i\tilde{k}_- \end{pmatrix} \begin{pmatrix} \psi^+(x) \\ \psi^-(x) \end{pmatrix} \tag{35}$$

The transfer matrix M that matches the state vector at two different locations is defined via the relation

$$\vec{\psi}(x_2) = M\vec{\psi}(x_1) \tag{36}$$

In a ring with a weak-link there are two segments with different diffusion coefficients D_0 and D_1. The continuity of the density $\rho(x)$ and the current $J = -D(x)\partial\rho(x) + v(x)\rho(x)$ implies that the derivative $\partial\rho$ should have a jump such that across the boundary

$$\left.\begin{pmatrix} \rho \\ \partial\rho \end{pmatrix}\right|_1 = \begin{pmatrix} 1 & 0 \\ 0 & D_0/D_1 \end{pmatrix} \left.\begin{pmatrix} \rho \\ \partial\rho \end{pmatrix}\right|_0 \tag{37}$$

We define the matrices

$$U = \begin{pmatrix} 1 & 1 \\ i\tilde{k}_+ & i\tilde{k}_- \end{pmatrix} \tag{38}$$

$$T = \begin{pmatrix} e^{i\tilde{k}_+ x} & 0 \\ 0 & e^{i\tilde{k}_- x} \end{pmatrix} \tag{39}$$

$$R = \begin{pmatrix} 1 & 0 \\ 0 & D_0/D_1 \end{pmatrix} \tag{40}$$

For free propagation over a distance L we have $M_0 = UT_0U^{-1}$, with T_0 that involves a wavenumber k that is determined by D_0. For a weak-link we have $M_1 = R^{-1}UT_1U^{-1}R$, where T_1 describes the free propagation in the D_1 region that has some thickness a. It is convenient to define the effective width of the weak link as $\ell = (D_0/D_1)a$. The only non-trivial way to take the limit of zero thickness weak-link ($a \to 0$) is to adjust $D_1 \to 0$ such that ℓ is kept constant. This leads to the following result:

$$M_1 = R^{-1}UT_1U^{-1}R = \begin{pmatrix} 1 & \ell \\ 0 & 1 \end{pmatrix} \tag{41}$$

The characteristic equation is

$$\det\left[1 - M_1M_0\right] = 0 \tag{42}$$

leading to

$$\cos(q) - \frac{1}{2g}\left[q^2 + \left(\frac{S_\circlearrowleft}{2}\right)^2\right] \frac{\sin(q)}{q} = \cosh\left(\frac{S_\circlearrowleft}{2}\right) \tag{43}$$

where we have defined

$$g \equiv \frac{L}{\ell} = \frac{L/D_0}{a/D_1} \tag{44}$$

along with $q = kL$ and $S_\circlearrowleft = sL$.

In Fig.4 we deduce the dependence of Γ on S and on g. In order to determine the threshold S_c for the appearance of complex eigenvalues we take a closer look at Eq. (43). The left hand side is an oscillating function within an envelope

$$A(q) \;=\; \sqrt{1+\frac{1}{g^2}\left(\frac{q^2+(S_\circlearrowleft/2)^2}{2q}\right)^2} \qquad (45)$$

This envelope has a minimum at $q = S_\circlearrowleft/2$. Accordingly if $A(S_\circlearrowleft/2) < \cosh(S_\circlearrowleft/2)$ complex eigenvalues appear, and we can deduce the threshold S_c from the equation

$$\sqrt{1+\left(\frac{S_\circlearrowleft}{2g}\right)^2} \;=\; \cosh\left(\frac{S_\circlearrowleft}{2}\right) \qquad (46)$$

To get an explicit expression we solve the approximated equation $S_\circlearrowleft/(2g) = \cosh(S_\circlearrowleft/2)$ and deduce a solution in terms of the Lambert function,

$$S_c \;=\; -2\mathbb{W}(-g/2) \qquad (47)$$

This is valid provided $S \gg g$, which is self-justified for small g. We can use the same procedure in order to determine the complexity threshold for a given eigenvalue λ in Fig. 3. Recall that the corresponding q is $q^2 = L^2\lambda/D_0 - S_\circlearrowleft^2/4$. Solving the quadratic equation $A(q) = \cosh(S_\circlearrowleft/2)$ we find the q beyond which the spectrum becomes real again. It terms of λ the explicit expression is

$$\lambda_c = \frac{2D_0}{L^2}g^2\sinh^2\left(\frac{S_\circlearrowleft}{2}\right)\left[1+\sqrt{1-\left(\frac{S_\circlearrowleft}{2g\sinh\frac{S_\circlearrowleft}{2}}\right)^2}\right] \qquad (48)$$

This boundary is indicated by a dashed black line in Fig.3).

VI. RECONSTRUCTION OF THE CONTINUUM LIMIT

By reverse engineering, requiring consistency between Eq. (43) and Eq. (22), we deduce that the electrostatic potential that is associated with the discretized version of the characteristic equation for a ring with a weak link is

$$V(\epsilon) = \ln\left\{2(\cos(q)-1) - \frac{1}{g}\left[q^2+\left(\frac{S_\circlearrowleft}{2}\right)^2\right]\frac{\sin(q)}{q}\right\} \qquad (49)$$

This potential is plotted in Fig.5, and labeled as "$N{=}\infty$". We would like to reconstruct this potential by means of Eq. (24). For this purpose we have to find the real eignevalues of the associated $\boldsymbol{H}$, see Eq. (B6). Formally the equation $\det(z+\boldsymbol{H}) = 0$ is obtained by setting $S_\circlearrowleft{=}0$ in the right hand side (RHS) of Eq. (43), leading to

$$\cos(q) - \frac{1}{2g}\left[q^2+\left(\frac{S_\circlearrowleft}{2}\right)^2\right]\frac{\sin(q)}{q} \;=\; 1 \qquad (50)$$

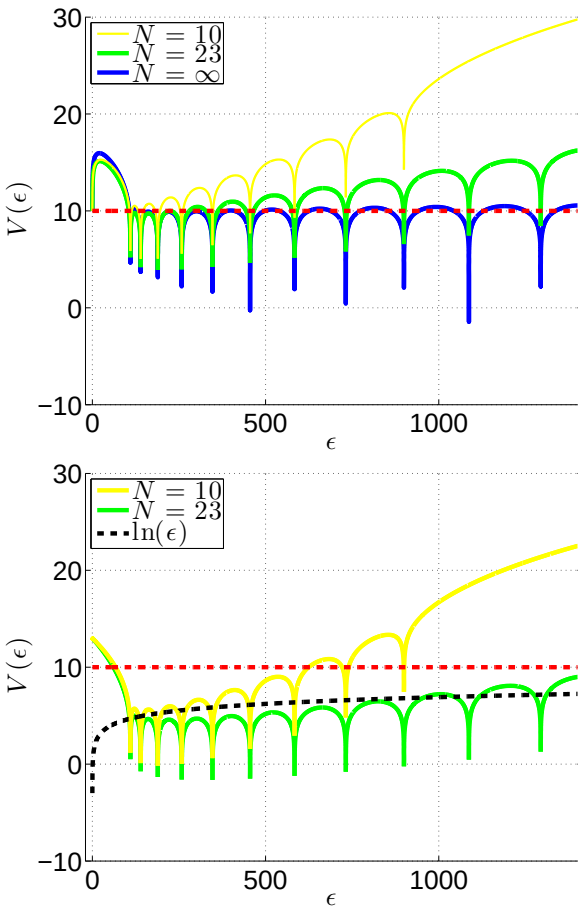

FIG. 5. Electrostatic reconstruction of the characteristic equation of a continuous ring with weak-link with $D = L = 1$ and $g = 10^{-3}$ and $S_\circlearrowleft = 20$. The blue line is the electrostatic potential of a continuous ring with a defect. The dashed red line is $V(0)$. The yellow and green lines are reconstructions using a finite number of (numerically obtained) charges. By increasing the number of charges that are included in the reconstruction, it is clear that the deviation from the blue line is due to finite size truncation. In the lower panel we display the contribution of the impurity-level charge (dashed black line) and the quasi-continuum charges (the other lines) to the reconstructed potential.

From Eq. (32) it follows that $\epsilon_k = \left[q_k^2 + S_\circlearrowleft^2/4\right] D_0/L^2$, where q_k are the roots of the above equation. Using these "charges" we compute $V(\epsilon)$ via Eq. (24) and plot the result in the upper panel of Fig. 5. Some truncation is required, so we repeat the attempted reconstruction with $N = 10$ and $N = 23$ roots. We observe that the result converges to the $N{=}\infty$ limit. The residual systematic error as ϵ becomes larger is due to finite truncation of the number of roots used in the reconstruction.

The characteristic, equation Eq. (43) parallels the discrete version Eq. (22). One should be aware that the spectral density contains an "impurity" charge ϵ_0 as illustrated in the third panel of Fig. 2. It is easy to explain the appearance of this exceptional charge using the

discrete-lattice language. In the absence of a weak link the diagonal elements of the $\boldsymbol{W}$ matrix are $-\gamma$ where $\gamma = we^{s/2} + we^{-s/2} = 2w\cosh s/2$. The spectrum of the associated $\boldsymbol{H}$ matrix forms a band, such that the lower edge of $\varrho(\epsilon)$ is

$$\epsilon_{\rm floor} \;=\; \gamma - 2w \;=\; 2w\,[\cosh(s/2) - 1] \qquad (51)$$

If we introduce a weak-link $w_0 \ll w$ at the $(0,1)$ bond, we get one exceptional diagonal element γ_0. Consequently, for small enough w_0, there is an out-of-band impurity level that does not mix with the band:

$$\epsilon_0 \;\approx\; \gamma_0 \;= w_0 e^{s/2} + we^{-s/2} \qquad (52)$$

In the lower panel of Fig.5 we separate the contribution of the impurity level from the contribution off all the other band-levels.

VII. DISCUSSION

We have outlined a physically appealing procedure to extract the relaxation rate of a stochastic spreading process in a closed ring, bridging between the discrete model and its continuum limit, and treating on equal footing full and sparse disorder. By sparse disorder we mean several weak-links. For presentation purposes we have provided a full analysis for a ring with a single defect, but the generalization to several weak links is merely a technical issue.

Our approach has been inspired by previous works regrding non-Hermitian Hamiltonians [13–15], and follows our previous publication [16] regarding the determination of the complexity threshold. In the present work the emphasis was on the determination of the relaxation rate Γ in the "complex" regime where the topological aspect manifests itself. Generally speaking in this regime Γ may exhibit anomalous dependence on the length of the sample.

Acknowledgements.– We thank Oleg Krichevsky (BGU) for a helpful discussion. This research has been supported by by the Israel Science Foundation (grant No. 29/11).

Appendix A: Expressions for v and D in the presence of disorder

In the presence of disorder, the forward and backward rates are random numbers. Here we summarize known analytical expressions for v and D based on [2], and notations as in [16–18]. Taking the infinite chain limit, and using units such that the lattice spacing is $a = 1$, the expression for the drift velocity is

$$v = \frac{1 - \left\langle \frac{\overleftarrow{w}}{\overrightarrow{w}} \right\rangle}{\left\langle \frac{1}{\overrightarrow{w}} \right\rangle} \tag{A1}$$

We notice that a non-percolating resistor-network-disorder will diminish the drift velocity as expected due to the denominator. Irrespective of that the result above is valid only in the "sliding regime" where $v > 0$. Looking at the numerator one observes that the implied condition for that is $s > s_1$. As for the diffusion, it becomes finite for $s > s_2$, and the explicit expression is

$$D = \frac{1 - \left\langle \frac{\overleftarrow{w}}{\overrightarrow{w}} \right\rangle^2}{1 - \left\langle \left(\frac{\overleftarrow{w}}{\overrightarrow{w}} \right)^2 \right\rangle} \left\langle \frac{1}{\overrightarrow{w}} \right\rangle^{-3} \times \left[\left\langle \frac{1}{\overrightarrow{w}} \right\rangle \left\langle \frac{\overleftarrow{w}}{\overrightarrow{w}^2} \right\rangle + \frac{1}{2} \left\langle \frac{1}{\overrightarrow{w}^2} \right\rangle \left(1 - \left\langle \frac{\overleftarrow{w}}{\overrightarrow{w}} \right\rangle \right) \right] \tag{A2}$$

For large bias a practical approximation is

$$D \approx \frac{1}{2} \left\langle \frac{1}{\overrightarrow{w}} \right\rangle^{-3} \left\langle \frac{1}{\overrightarrow{w}^2} \right\rangle \tag{A3}$$

Considering a ring with random rates $we^{\pm \mathcal{E}_n/2}$, the dependence of all the various expectation values on the affinity s is expressible in terms of the parameters w and s_μ. For example

$$v = e^{\frac{1}{2}(s_1 - s_{1/2})} \left[2 \sinh \left(\frac{s - s_1}{2} \right) \right] w \tag{A4}$$

Appendix B: The associated H matrix

Our model is described by a conservative matrix $\boldsymbol{W}$ that describes hopping between sites. In the Chain configuration the site index n runs from $-\infty$ to ∞, while in the Ring configuration it is defined modulo N. In the latter case we characterize the stochastic field by a potential $U(n)$ and by an affinity $S_\circlearrowleft$, such that

$$\mathcal{E}_n = U(n) - U(n-1) + \frac{S_\circlearrowleft}{N} \tag{B1}$$

Then we associate with $\boldsymbol{W}$ a similar matrix $\tilde{\boldsymbol{W}}$ and a real symmetric matrix $\boldsymbol{H}$ as follows:

$$\boldsymbol{W} = \text{diagonal}\Big\{ -\gamma_n(s) \Big\} + \text{offdiagonal}\Big\{ w_n e^{\pm \frac{\mathcal{E}_n}{2}} \Big\}$$
$$\tilde{\boldsymbol{W}} = \text{diagonal}\Big\{ -\gamma_n(s) \Big\} + \text{offdiagonal}\Big\{ w_n e^{\pm \frac{S_\circlearrowleft}{2N}} \Big\}$$
$$\boldsymbol{H} = \text{diagonal}\Big\{ -\gamma_n(s) \Big\} + \text{offdiagonal}\Big\{ w_n \Big\}$$

such that

$$\tilde{\boldsymbol{W}} = e^{\boldsymbol{U}/2} \boldsymbol{W} e^{-\boldsymbol{U}/2} \tag{B2}$$

where $\boldsymbol{U} = \text{diag}\{U(n)\}$ is a diagonal matrix. The relation between $\boldsymbol{W}$ and $\tilde{\boldsymbol{W}}$ can be regarded as a gauge transformation, and $S_\circlearrowleft$ can be regarded as an imaginary Aharonov-Bohm flux. The hermitian matrix $\boldsymbol{H}$ can be regarded as the Hamiltonian of a particle in a ring in the absence of a magnetic flux. The $\boldsymbol{W}$ of a clean ring Eq. (3) and its associated $\boldsymbol{H}$ are

$$\boldsymbol{W} = 2w \left[\cos\left(\boldsymbol{P} + i\frac{s}{2} \right) - \cosh\left(\frac{s}{2} \right) \right] \tag{B3}$$
$$\boldsymbol{H} = 2w \left[\cos\left(\boldsymbol{P} \right) - \cosh\left(\frac{s}{2} \right) \right] \tag{B4}$$

while in the continuum limit Eq. (7) implies that

$$\boldsymbol{W} = -D\boldsymbol{P}^2 + iv\boldsymbol{P} \tag{B5}$$
$$\boldsymbol{H} = -D \left[\boldsymbol{P}^2 + \left(\frac{v}{2D} \right)^2 \right] \tag{B6}$$

In the absence of disorder the eignevalues are obtained by the simple substitution $\boldsymbol{P} \mapsto (2\pi/L)\nu$, where ν is an integer.

Appendix C: The characteristic equation

Consider the tridiagonal matrix

$$\boldsymbol{A} = \begin{pmatrix} a_0 & b_1 & 0 & ... & c_0 \\ c_1 & a_1 & b_2 & ... & 0 \\ 0 & c_2 & a_2 & ... & 0 \\ ... & ... & ... & ... & ... \\ b_0 & 0 & 0 & ... & 0 \end{pmatrix} \tag{C1}$$

and associated set of transfer matrices

$$T_n = \begin{pmatrix} a_n & -b_n c_n \\ 1 & 0 \end{pmatrix} \tag{C2}$$

Our modified indexing scheme of the elements, allows a simpler presentation of the formula for the determinant that appears in [19]:

$$\det[\boldsymbol{A}] = \text{trace} \left[\prod_{n=1}^{N} T_n \right] - (-1)^N \left[\prod_{n=1}^{N} b_n + \prod_{n=1}^{N} c_n \right]$$

From here follows

$$\det(z + \boldsymbol{W}) = \det(z + \tilde{\boldsymbol{W}}) = \det(z + \boldsymbol{H}) - 2 \left[\cosh\left(\frac{S_\circlearrowleft}{2} \right) - 1 \right] (-w)^N \tag{C3}$$

Hence the characteristic equation is Eq. (22).

Appendix D: The spectral density $\varrho(\epsilon)$

Consider a ring where the transition rates between neighboring sites are random variables $we^{\pm\mathcal{E}_n/2}$. The equation that describes the relaxation in such a ring in the continuum limit is Eq. (7) with "white disorder". Namely $v(x)$ has Gaussian statistics with $\langle v(x)v(x')\rangle = \nu_\sigma\delta(x-x')$ where $\nu_\sigma = w^2a^3\mathrm{Var}(\mathcal{E})$. Assuming $D(x) = D_0$, and adding to the disorder an average value v_0, one observes that the diffusion equation is characterized by a single dimensionless parameter. It is customary to define

$$\mu \equiv \frac{2D_0}{\nu_\sigma}v_0 = \frac{2s}{\mathrm{Var}(\mathcal{E})} \tag{D1}$$

This parameter equals v_0 if we use the common re-scaling of units such that $2D_0 = \nu_\sigma = 1$. Then the units of time and of length are

$$[T] = \frac{8D_0^3}{\nu_\sigma^2} = \left[\frac{8}{\mathrm{Var}(\mathcal{E})^2}\right] w^{-1} \tag{D2}$$

$$[L] = \frac{4D_0^2}{\nu_\sigma} = \left[\frac{4}{\mathrm{Var}(\mathcal{E})}\right] a \tag{D3}$$

In the absence of disorder, by inspection of Eq. (B6), the spectral density $\varrho(\epsilon)$ is like that of a "free particle" but shifted upwards such that the band floor is $\epsilon_0 = (1/4)v^2/D$. In the presence of Gaussian disorder the gap $[0,\epsilon_0]$ is filled. In scaled units the integrated density of states is [3]:

$$\mathcal{N}(\epsilon) = \frac{1}{\pi^2}\frac{L}{J_\mu^2(\sqrt{2\epsilon})+Y_\mu^2(\sqrt{2\epsilon})} \tag{D4}$$

where J_μ and Y_μ are Bessel functions of the first and second kind. For any μ the large asymptotics gives $\mathcal{N}(\epsilon) \approx (1/\pi)\sqrt{2\epsilon}$ in agreement with the free particle result. In the other extreme, for small ϵ we get $\mathcal{N}(\epsilon) \propto \epsilon^\mu$. It is also not difficult to verify that the clean ring spectrum (with its gap) is recovered in the $\sigma \mapsto 0$ limit.

We have verified that for box-distributed $\mathcal{E}_n$ the approximation $\varrho(\epsilon) \propto \epsilon^{\mu-1}$ holds at the vicinity of the band floor. In contrast with a Gaussian distribution μ becomes infinite as s approaches $s_\infty = \sigma$, see Eq. (18). For $s > s_\infty$ a gap is opened.

Appendix E: Step by step electrostatics

The eigenvalues ϵ_n of $\boldsymbol{H}$ can be regarded as the locations of charges in a 2D electrostatic problem. We would like to gain some intuition for the associated potential along the real axis. For a point charge at ϵ_1 we have $V(\epsilon) = \ln|\epsilon-\epsilon_1|$. For a uniform charge distribution within $\epsilon \in [a,b]$ we get

$$V(\epsilon) = \frac{1}{b-a}\int_a^b \ln|\epsilon-\epsilon'|\,d\epsilon' \tag{E1}$$
$$= \frac{1}{b-a}\left[(\epsilon-a)\ln|\epsilon-a| - (\epsilon-b)\ln|\epsilon-b| + (a-b)\right]$$

which has a minimum at $\epsilon = (a+b)/2$ and resembles a "soft well" potential. In order to have a flat floor the density has to be larger at the edges. This is the case for a charge density that corresponds to the spectrum of a clean ring. The locations of the charges are

$$\epsilon_n = 2\left[\cosh\left(\frac{s}{2}\right) - \cos\left(\frac{2\pi}{N}n\right)\right] \equiv \epsilon(k_n) \tag{E2}$$

and the potential along the real axis is

$$V(\epsilon) = \frac{N}{2\pi}\int_0^{2\pi}\ln|\epsilon-\epsilon(k)|\;dk \tag{E3}$$

For ϵ within the band, the integrand can be written as $\ln|2(\cos(k_0)-\cos(k))|$, and accordingly the potential vanishes, reflecting an infinite localization length.

In the continuum limit the charge density in the case of a clean ring behaves as $\varrho(\epsilon) \propto \epsilon^{\mu-1}$ with $\mu = 1/2$ and leads to a flat floor. For general μ one can show [16] that

$$V'(\epsilon) \propto \pi\mu\cot(\pi\mu)\;\epsilon^{\mu-1} \tag{E4}$$

such that the sign of $V'(\epsilon)$ is positive for $\mu < 1/2$, and negative for $\mu > 1/2$. See Fig.2 for an illustration. We also illustrate there what happens if we have a clean ring that is perturbed by a defect that contributes a charge in the gap.

For $s > s_\infty$ we have $\mu = \infty$, meaning that a gap is opened. If s is sufficiently large the eigenstates of $\boldsymbol{H}$ are "trivially localized", so the eigenvalues are simply

$$\epsilon_n = \exp[(s+\varsigma_n)/2] \tag{E5}$$

where $\varsigma_n \in [-\sigma,\sigma]$ is uniformly distributed. Accordingly the charge density is $\varrho(\epsilon) = N/\sigma\epsilon$ within an interval $\epsilon \in [a,b]$, where $a = \exp[(s-\sigma)/2]$ and $b = \exp[(s+\sigma)/2]$, leading to

$$V(\epsilon) = \frac{N}{\sigma}\left[\ln(|\epsilon-a|)\ln\left(\frac{\epsilon}{a}\right) - \ln(|\epsilon-b|)\ln\left(\frac{\epsilon}{b}\right) + \mathrm{Li}_2\left(1-\frac{a}{\epsilon}\right) + \mathrm{Li}_2\left(1-\frac{b}{\epsilon}\right)\right] \tag{E6}$$

We would like to calculate the decay rate as described by Eq. (30). To carry out the calculation it is easier to integrate with respect to ς. Expanding Eq. (25) in the vicinity of the origin we get the coefficients

$$C_1 = \frac{N}{2\sigma}\int_{-\sigma}^{\sigma} e^{-(s+\varsigma)/2}d\varsigma$$
$$= \frac{2N}{\sigma}\sinh\left(\frac{\sigma}{2}\right)e^{-s/2} = Ne^{(s_{1/2}-s)/2} \tag{E7}$$

$$C_2 = \frac{N}{2\sigma}\int_{-\sigma}^{\sigma} e^{-(s+\varsigma)}d\varsigma$$
$$= \frac{N}{\sigma}\sinh(\sigma)e^{-s} = Ne^{s_1-s} \tag{E8}$$

Substitution of C_1 and C_2 into Eq. (30) leads to a result that agrees with Eq. (21).

[1] Y. G. Sinai, Theor. Probab. Appl. **27**, 256 (1983), http://dx.doi.org/10.1137/1127028.
[2] B. Derrida, J. Stat. Phys. **31**, 433 (1983).
[3] J. Bouchaud, A. Comtet, A. Georges, and P. L. Doussal, Ann. Phys. **201**, 285 (1990).
[4] J.-P. Bouchaud and A. Georges, Phys. Rep. **195**, 127 (1990).
[5] D. R. Nelson and N. M. Shnerb, Phys. Rev. E **58**, 1383 (1998).
[6] K. A. Dahmen, D. R. Nelson, and N. M. Shnerb, in *Statistical mechanics of biocomplexity* (Springer Berlin Heidelberg, 1999) pp. 124–151.
[7] D. K. Lubensky and D. R. Nelson, Phys. Rev. Lett. **85**, 1572 (2000).
[8] D. K. Lubensky and D. R. Nelson, Phys. Rev. E **65**, 031917 (2002).
[9] M. E. Fisher and A. B. Kolomeisky, P. Natl. Acad. Sci. USA **96**, 6597 (1999).
[10] M. Rief, R. S. Rock, A. D. Mehta, M. S. Mooseker, R. E. Cheney, and J. A. Spudich, P. Natl. Acad. Sci. USA **97**, 9482 (2000).
[11] Y. Kafri, D. K. Lubensky, and D. R. Nelson, Biophys. J. **86**, 3373 (2004).
[12] Y. Kafri, D. K. Lubensky, and D. R. Nelson, Phys. Rev. E **71**, 041906 (2005).
[13] N. Hatano and D. R. Nelson, Phys. Rev. Lett. **77**, 570 (1996).
[14] N. Hatano and D. R. Nelson, Phys. Rev. B **56**, 8651 (1997).
[15] N. M. Shnerb and D. R. Nelson, Phys. Rev. Lett. **80**, 5172 (1998).
[16] D. Hurowitz and D. Cohen, Scientific Reports **6**, 22735 (2016).
[17] D. Hurowitz, S. Rahav, and D. Cohen, Phys. Rev. E **88**, 062141 (2013).
[18] D. Hurowitz and D. Cohen, Phys. Rev. E **90**, 032129 (2014).
[19] L. G. Molinari, Linear Algebra Appl. **429**, 2221 (2008).